Available online at www.ijpe-online.com

International Journal of Performability Engineering

vol. 15, no. 3, March 2019, pp. 1005-1013
DOI: 10.23940/ijpe.19.03.p30.10051013

Specific Emitter Identification based on Power Amplifier

Zhen Zhang, Jie Chang*, Mengqiu Chai, and Nan Tang

Harbin Engineering University, Harbin, 150001, China

Abstract

Specific emitter identification is the process of identifying or discriminating different emitters based on the radio frequency fingerprints extracted from the received signal. Due to the inherent non-linearities of the power amplifiers of emitters, these features are extracted from the power amplifiers for specific emitter identification. In this paper, we take the 433MHz power amplifier module BLT54A as the research object, eight circuit modules with the same specifications and batches were tested. The experimental contents include: S parameters, AM-AM curve, AM-PM curve, input power and output power curve, AM-AM curve when bias voltage is different, AM-PM curve and input power and output power curve. We extract the energy characteristics of the HHT spectrum of the amplifier output signal and recognize it by classifier. The results show that the eight amplifiers can reach 75%. Meanwhile, we evaluate performance of specific emitter identification in several aspects including different signal sample length and different SNR.

Keywords: cognitive radio; cooperative spectrum sensing; spectrum sensing data falsification; defense reference

(Submitted on November 2, 2018; Revised on December 3, 2018; Accepted on January 5, 2019)

1. Introduction

The concept of individual identification of radiation sources can be traced back to the identification of telegraph key fingerprints during World War II. In an age when computer technology has not flourished, individual identification is done primarily through well-trained or talented people. In the mid-1960s, the US military officially proposed the need for individual identification of radiation sources for the purpose of indicating mobile communication transmitters. As the demand evolved, the concept of SEI was gradually formed [1].

Since the 1990s, western military powers, especially the United States, have made great progress in the identification of individual radiation sources, and the military has continued to fund relevant institutions to conduct research to maintain its leading position. The US Naval Laboratories, Northrop Grumman, Litton, Applied Signals, and British QinetiQ have long-term technical research and systems development experience with SEI. In particular, Northrop Grumman has been researching this technology for more than 40 years, leading or participating in the development of a range of military and civilian SEI systems and systems containing SEI functions, including the ALR-95 (V) Type 1 developed for the EP-3C, the ALQ-217 electronic support system developed for E-2C and the AN/SLQ-32(V) electronic support system. Europe's systems with individual identification capabilities include the VERA-E (Vera) system in the Czech Republic and the CELT Mariner RWR marine alarm in the UK [2-3].

Domestic individual identification research began in the 1990s when the SEI technology of the United States made great progress. At that time, a number of research institutions tracked public reports abroad, and extensively discussed the concepts of radar signal fingerprinting, intrapulse analysis, accurate parameter measurement and individual identification of radiation sources and possible methods [4]. However, no detailed research has been done on the individual characteristics of the radiation source.

Common Radiation Source RF signals are mainly composed of three parts: channel noise segment, transient signal segment, and steady state signal segment. The channel noise segment refers to a signal segment in which the receiver does

* Corresponding author.
E-mail address: changjie@hrbeu.edu.cn

not acquire a communication signal, and is mainly composed of channel noise and device noise. The transient signal segment refers to the signal segment transmitted when the transmitter power reaches the rated power from zero. This signal does not contain data information, and is only related to the hardware characteristics of the device itself, and can be used as an identifiable signal to extract the radio frequency fingerprint feature. The steady state signal segment refers to the portion of the signal transmitted by the wireless transmitter under power stability. According to the class of identifiable signals, individual identification of radiation sources can be divided into two categories: transient identification and steady state identification.

Transient signals include switching machine transients, where startup transients are the most widely studied. It mainly includes transient feature extraction based on time-frequency analysis, wavelet theory, fractal theory and chaos theory.

Steady state signals are sometimes difficult to account for the physical meaning of the features. However, there are indeed differences in the subtleties of intentionally modulated signals. This difference has some stability and observability, and sometimes even can be seen with the naked eye.

Unintentional modulation (UM) can be represented by a modulation curve. Langley [5] pointed out that unintentional frequency modulation (UMOF) is an important feature of specific radiation source identification. He used the example data of commercial radars and navigation radars to compare the intrapulse modulation curves of different radiation source individuals and proposed to combine this feature with the identification method of a traditional parameter fusion. Liu Zheng [6] also made a detailed experimental study on the performance of UMOF in pulse signal classification. The infield experiment approached the practical index under the condition that the training sample was sufficient. Zhang Guozhu et al. [7] studied the unintentional amplitude modulation (UMOA) from the video envelope of the signal. In 2007, T. of the US Naval Laboratory L. Carroll [8] proposed a nonlinear dynamic SEI method in Chaos magazine for fingerprint extraction of radiation source power amplifiers. This paper points out the limitations of its approach: the excitation signals of amplifiers from different sources must be close enough. This discussion of limitations reflects the common problems in fingerprint research at home and abroad: the lack of independence of features. When the intentional modulation changes, the classification ability will drop sharply. In 2008, Xudan proposed the fingerprint analysis of power amplifier based on blind identification of nonlinear systems and studied the power amplifier fingerprint recognition technology under the excitation of variable power monophonic sinusoidal signal excitation, narrowband signal excitation and modulation wideband signal excitation. For the three kinds of signals, he proposed the harmonic constraint feature based on Wu Wenjun's method, the Taylor series model based on narrowband signal model and power amplifier, and the Volterra series model based on power amplifier. On this basis, he also carried out simulation experiments and analyzed the independence and measurability of fingerprints [9-10].

2. Basic Theory

2.1. Nonlinear Amplification of Amplifiers

The Taylor model of the power amplifier regards the amplifier as an instantaneous non-linear function and describes it in the form of a series. In narrowband condition, a Taylor series model with high order is sufficient to describe the nonlinear characteristics of amplifier [11].

The Taylor series model is based on a narrowband excitation signal. The general form of narrowband signal is:

$$u(t) = r(t)\cos(2\pi f_0 t + \theta) \tag{1}$$

$r(t)$ is the baseband envelope of the signal $u(t)$, f is the carrier frequency, and θ is the arbitrary initial phase. The output of the amplifier can be recorded as:

$$y(t) = O\{u(t)\} \tag{2}$$

The $O\{\cdot\}$ is the overall modulation characteristic of the amplifier. It consists of an AM-AM transfer function and AM-PM transfer function. Let $O\{u(t)\}$ expand to $u(t)$ Taylor expansion and get the Taylor series model of the RF amplifier.

$$y(t) = \sum_{n=0}^{\infty} a_n u^n(t) \tag{3}$$

When the model is used to analyze the unintentional modulation of the whole spectrum, both odd and even power terms need to be considered. If only unintentional modulation in the working frequency band of the signal is analyzed, even power terms can be ignored because even power terms are generated. The signal component is always far away from the working frequency band. The Taylor series model does not assign any part of the subsequent linear system.

Assuming that, for simplicity, the various Doppler and multipath effects of the linear part and the wireless channel are not taken into account here for the time being. The general expression of harmonic amplitude and phase should be derived directly from the Taylor series model, and the excitation signal should be studied.

The excitation signal of the power amplifier is an ideal sinusoidal signal, and the Taylor series model is truncated. The simple case of order 3 is studied.

When the order of amplifier model is 3, the excitation signal represented by formula (1) is $r(t) = A,\ \omega = 2\pi f_0$, and the output signal $y(t)$ can be expressed as follows.

$$y(t) = a_0 + a_1 A\sin(\omega t+\theta)+\mathrm{a}_2 A^2 \sin^2(\omega t+\theta) + a_3 A^3 \sin^3(\omega t+\theta) \tag{4}$$

After trigonometric function expansion and simple derivation, the expression of the relative value $A_1^{(r)}$ of the component amplitude of the first frequency multiplication to the carrier frequency component amplitude can be obtained as follows.

$$A_2^{(r)} = \log(a_2 A^2) - \log(2(a_1 A + \frac{3}{4} a_3 A^3)) \tag{5}$$

$$A_3^{(r)} = \log(a_3 A^3) - \log(4(a_1 A + \frac{3}{4} a_3 A^3)) \tag{6}$$

It can be seen that the relative amplitude of each harmonic is a function of the amplitude of the excitation signal. Because the energy of harmonics in $y(t)$ is much less than that of the carrier wave.

$$a_1 A >> a_3 A^3 \tag{7}$$

The following formulas are obtained by approximation of Formulas (5) and (6)

$$2A_2^{(r)} - A_3^{(r)} \approx C \tag{8}$$

Among them, C is a constant, and the upper formula is approximated to a linear constraint on the plane. Thus, under certain conditions, the characteristic parameters independent of the excitation signal amplitude *A* can be obtained from the relative harmonic amplitude.

2.2. Hilbert-Huang Transform

HHT is an adaptive tool which can be applied to non-linear and non-stationary signals. The main content of HHT consists of two parts. The first part is Empirical Mode Decomposition (EMD). The second part is the Hilbert Spectrum Analysis (HSA). The former is a sifting process to decompose any signal into an infinite set of intrinsic mode function (IMF), while the latter offers the time-frequency distribution, referred to as the Hilbert spectrum, by performing the Hilbert transform on each IMF [12-13].

2.2.1. Empirical Mode Decomposition

EMD is often referred to as a “screening” process. This filtering process adaptively decomposes any complex signal into a series of intrinsic mode functions (IMFs) according to the characteristics of the signal. It satisfies the following two conditions [14]:

a) The number of signal extremum points is equal to or different from zero points.

b) The local mean of the upper envelope defined by the maximum and the lower envelope defined by the minimum of the signal is zero.

Take $z(t)$ as the original signal The EMD screening process is as follows:

i) Identify all local maxima and minima to obtain the upper and lower envelopes by cubic spline fitting, where the signal is covered between the upper and lower envelopes;

ii) Calculate the mean of the upper and lower envelopes, denoted by $\mu_{10}(t)$. The first component $z_{10}(t)$ is defined as the difference between $z(t)$ and $\mu_{10}(t)$, $z_{10}(t) = z(t) - \mu_{10}(t)$;

iii) Repeat steps i) and ii) p times until $z_{1p}(t)$ becomes an IMF

$$z_{1p}(t) = z_{1(p-1)}(t) - \mu_{1p}(t), \quad p = 1,\ 2,\ \cdots \tag{9}$$

where $\mu_{1p}(t)$ is the mean of the upper and lower envelopes of $z_{1(p-1)}(t)$. The stopping criterion is when

$$\xi = \sum_{t=0}^{T_S} \frac{| z_{1(p-1)}(t) - z_{1p}(t) |^2}{z_{1(p-1)}^2(t)} \tag{10}$$

is below a predefined value ε, with T_s as the length of the signal1;

iv) Let $c_1(t) = z_{1p}(t)$ be the first IMF; this is subtracted from $z(t)$ to obtain the residual

$$d_1(t) = z(t) - c_1(t) \tag{11}$$

The residual, containing the IMF, is considered as a new signal to implement the sifting process;

v) Repeat steps i) to iv) on all residuals $d_q(t)$, q = 1, ⋯, Q, with Q as the number of IMFs, and $d_q(t)$

$$\begin{aligned} d_2(t) &= d_1(t) - c_2(t) \\ &\vdots \\ d_Q(t) &= d_{Q-1}(t) - c_Q(t) \end{aligned} \tag{12}$$

The sifting process is stopped when either $d_Q(t)$ is less than the predefined value of ξ or becomes a monotonic function, which contains no oscillation.

From (11) and (12), $z(t)$ can be expressed as

$$z(t) = \sum_{q=1}^{Q} c_q(t) + d_Q(t) \tag{13}$$

2.2.2. Hilbert Spectrum Analysis

Hilbert transform $y(t)$ can be expressed as $z(t)$ of any time series.

$$y(t) = \frac{1}{\pi} \int_{-\infty}^{+\infty} \frac{z(\tau)}{t - \tau} \mathrm{d}\tau \tag{14}$$

Constructing analytic functions:

$$x(t) = z(t) + iy(t) = a(t)e^{i\theta(t)} \tag{15}$$

$a(t)$ and $\theta(t)$ are respectively called instantaneous amplitude and phase of signal $z(t)$.

$$a(t) = \sqrt{z^2(t) + y^2(t)} \tag{16}$$

$$\theta(t) = \arctan\frac{y(t)}{x(t)} \tag{17}$$

The instantaneous frequency of the signal obtained from the instantaneous phase is:

$$\omega(t) = \mathrm{d}\theta(t)/\mathrm{d}t \tag{18}$$

After Hilbert transform, each IMF component can be transformed into the instantaneous amplitude and frequency corresponding to the time variable of the signal. Because Hilbert transform requires high local characteristics, the false components of the analyzed signal in frequency domain should be removed. Taking time and frequency as independent variables and amplitude as dependent variables, the Hilbert amplitude spectrum $H(\omega,t)$ can be obtained.

$$H(\omega,t) = \mathrm{Re}\sum_{j=1}^{n} a_j(t)e^{\int 1/\omega^j(t)\mathrm{d}t} \tag{19}$$

Hilbert marginal spectrum $h(\omega)$ is defined as:

$$h(\omega) = \int_{-\infty}^{+\infty} H(\omega,t)\mathrm{d}t \tag{20}$$

Hilbert instantaneous energy is defined as:

$$IE(t) = \int_{\omega} H^2(\omega,t)\mathrm{d}\omega \tag{21}$$

Hilbert energy spectrum is defined as:

$$ES(\omega) = \int_0^T H^2(\omega,t)\mathrm{d}t \tag{22}$$

The above process is the Hilbert-Huang transform (HHT). The marginal spectrum provides the total amplitude corresponding to each frequency value, which means the distribution of energy accumulation at each frequency point in the whole time span.

$$z(t) = \sum_{r=1}^{p} a_r z(t-r) + e(t) \tag{23}$$

3. Individual Difference Analysis of Amplifiers

3.1. Measurement of Basic Characteristic of Amplifier

In this paper, we take the 433MHz power amplifier module BLT54A as the research object. Eight circuit modules with the same specifications and batches were tested. The experimental contents include: S parameters, AM-AM curve, AM-PM curve, input power, and output power curve, AM-AM curve when bias voltage is different, AM-PM curve and input power and output power curve.

Power amplifiers have many basic indicators to evaluate the performance of amplifiers. S-parameter curves and gain

compression curves are the basic indexes of amplifier. When studying the nonlinearity of amplifier, we usually observe the AM-AM characteristic curve and AM-PM characteristic curve of amplifier. Figure 1 shows the amplifier under test in this paper.

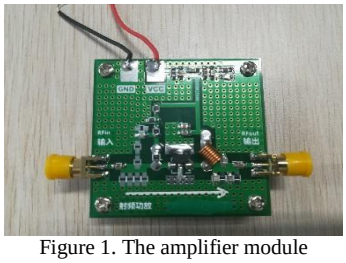

Figure 1. The amplifier module

Figure 2 shows S-parameter curve of the eight power amplifiers. Figure 3 shows the gain compression of eight power amplifiers. It shows that there are differences between eight power amplifiers which are from the same batch and same manufacturer. The results show that the power amplifier can be used for Specific Emitter Identification. In the real communication system, people use receivers to intercept and capture the output signals of enemy wireless devices. Therefore, in this paper, the output signal of the power amplifiers is collected for Specific Emitter Identification.

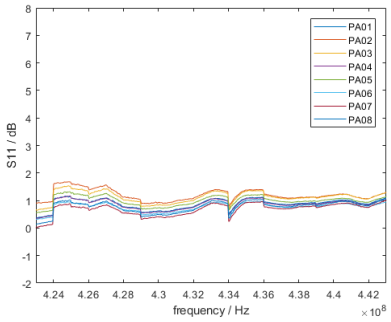

Figure 2. The S-parameter of eight amplifier

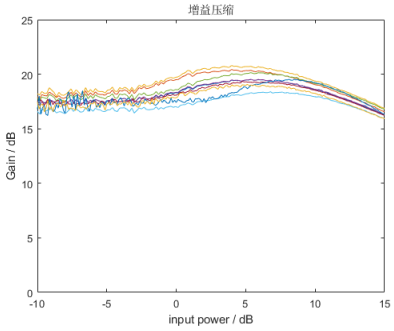

Figure 3. The gain compression curve of eight amplifier

Figure 4 shows the AM-AM characteristic curve and AM-PM characteristic curve of the eight amplifiers. Specific emitter identification is the process of identifying or discriminating different emitters based on the radio frequency fingerprints extracted from the received signal of the power amplifiers. Due to the inherent non-linearities of the power amplifiers, these features provide distinguishing features for individual identification. A static non-linearity can be determined from AM-AM characteristic curves and AM-PM characteristic curves. The results show that there are differences between the eight power amplifiers which are from the same batch and same manufacturer. The results show that the power amplifier can be used for Specific Emitter Identification.

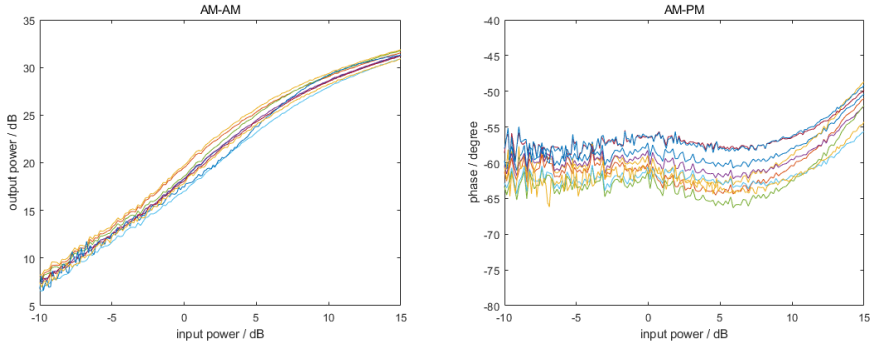

Figure 4. The AM-AM curve and AM-PM curve of eight amplifiers

3.2. Data Acquisition for Individual Recognition

In this paper, we use the BLT53A amplifier module as the research object. BLT53A is a power amplifier based on silicon technology, providing wide bandwidth operation support from DC to 3G. Designed for ultra-thin, ultra-small SOT89 packages, BLT53A provides complete internal matching with input and output approaching 50 ohms. BLT53A has a very

high efficiency. The power efficiency reaches 65% when the amplifier outputs 36dBm (3W) at 6V power supply and 433MHz operating frequency. BLT53A is very suitable for some data transmission systems. In some specific occasions, 2W communication power may be required, such as meter reading handset, security, hydrological measurement and control, aeromodelling and other applications. The working condition parameters of the amplifier are shown in Table 1. The data acquisition method and the experimental process are shown in Figure 5.

Table 1. Description of Amplifier Test Parameters

Parameter	**Index**
Carrier frequency	433MHz
Power voltage	5V
Power input	0dBm
Signal modulation mode	16QAM
Signal rate	2M
Signal bandwidth	1MHz
Sample rate	10MSa/s

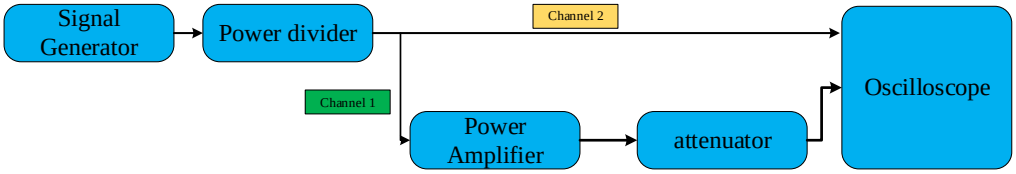

Figure 5. The data acquisition method

4. Simulation Results and Discussion

In this section, we investigate the specific emitter identification method based on HHT. We evaluate performance of specific emitter identification in several aspects. In this paper, we investigated the case of different signal sample lengths. The performance of the method is evaluated in terms of probability of identifying an output signal as a received signal from a power amplifier. Simultaneously, we show the feature of the eight amplifiers.

4.1. Different Signal Sample Length

To illustrate the feasibility and practicability of the features extracted from the output signal of the eight amplifiers, we consider different signal sample lengths including 5000, 10000, and 20000. Actually, people expect to distinguish the emitter from less data. It is worth noting that we intend to identify the emitters by obtaining the emitter-specific RF fingerprints from less samples. Figure 6 shows that the feature visualization with different signal sample lengths.

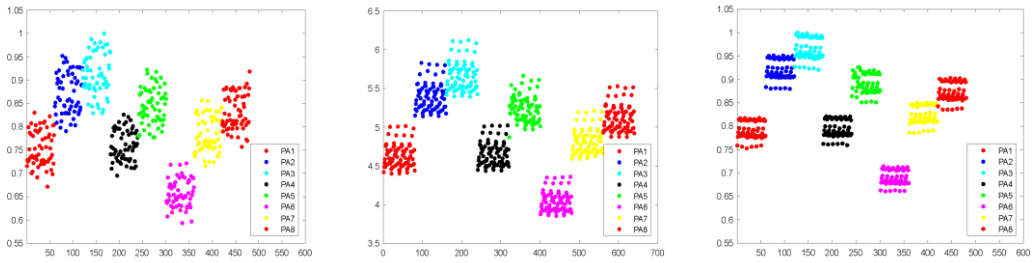

Figure 6. The feature visualization with different signal sample length

4.2. Different SNR

In communication systems, signal-to-noise ratio (SNR) is often considered, so it is necessary to analyze the performance of the feature extraction algorithm under different SNRs. From the above analysis of sample points, we can see that when the number of sample points is 20,000, the recognition effect should be the best. In the analysis of signal-to-noise ratio (SNR), we selected 20,000 samples as the research object. Using the method of controlling variables, the influence of signal-to-noise ratio on fine features is analyzed when the number of samples is the same.

Characteristic visualization under nine SNR conditions is shown in Figure 7 from -30dB to 30dB, we can see that with the increase of signal-to-noise ratio, the fine characteristics of amplifier become more and more obvious. The feature of the same individual is more and more dense, so it is more conducive to recognition.

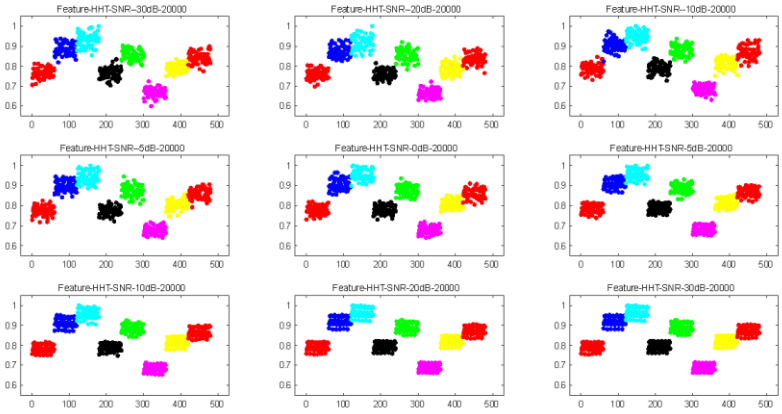

Figure 7. Characteristic visualization under nine SNR conditions

The recognition rate curves under nine signal-to-noise ratios are shown in Figure 8. After obtaining the above minute features, the KNN classifier is used to recognize them. The reason for using the KNN classifier is that KNN has less computational complexity in training and validating the individual recognition effect of the extracted fine features. In the experiment, we randomly allocate the extracted feature data set as the training data set in 70% proportion, and the rest as the test data set. Twenty experiments were carried out under the same signal-to-noise ratio, and 20 recognition rates were obtained. Finally, nine recognition rates were obtained, each of which had 20 recognition rates. We use the box diagram method to visualize it. As can be seen from the figure, with the increase of signal-to-noise ratio, the recognition rate is improving. From the box diagram, we can also see the maximum, minimum and median recognition rates of 20 times under each SNR. At the same time, we can see that each time the feature data is randomly allocated, the classification results are different, and different recognition rates will be obtained. Therefore, the distribution of feature data will also affect the recognition rate. In this experiment, we separated the feature dataset according to the 70% and 30% ratio. We deduced that different ratios would also affect the recognition rate. We also compared the confusion matrix of eight amplifiers under high and low SNR conditions. It can be seen that under the condition of high SNR, the recognition accuracy is better than that of low SNR. Figure 9 shows the confusion matrix under high signal-to-noise ratio and Figure 10 shows the confusion matrix under low signal-to-noise ratio.

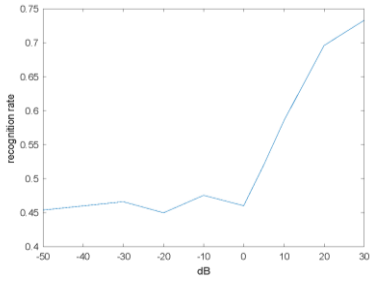

Figure 8. The recognition rate curves under nine signal-to-noise ratios

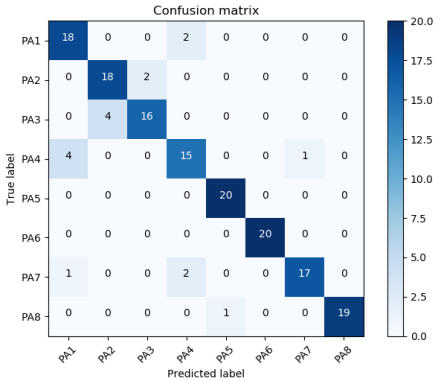

Figure 9. Confusion matrix under high signal-to-noise ratio

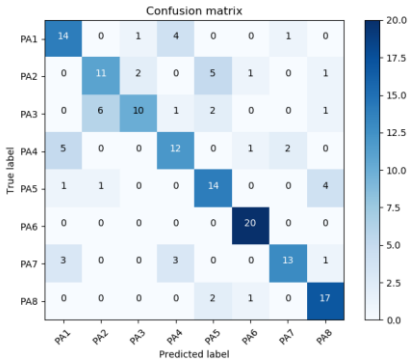

Figure 10. Confusion matrix under low signal-to-noise ratio

5. Conclusions

In this paper, we take the 433MHz power amplifier module BLT54A as the research object. Eight circuit modules with the same specifications and batches were tested. The experimental contents include: S parameters, AM-AM curve, AM-PM curve, input power, and output power curve, AM-AM curve when bias voltage is different, AM-PM curve and input power and output power curve. The results show that there are differences between eight power amplifiers which are from the same batch and same manufacturer. The results show that the power amplifier can be used for Specific Emitter Identification. We investigate the specific emitter identification method based on HHT. We evaluate performance of the specific emitter identification in several aspects. In this paper, we investigated the case of different signal sample lengths. The performance of the method is evaluated in terms of probability of identifying output signal as a received signal from a power amplifier. In the future, we can consider more kinds of amplifiers and more obvious features to identify individual emitters.

References

1. S. Cripps, "RF Power Amplifiers for Wireless Communications," MA, Artech House, Boston, 2006
2. A. A. M. Saleh, "Frequency-Dependent and Frequency-Independent Nonlinear Models of TWT Amplifiers," *IEEE Transactions on Communications*, Vol. COM-29, No. 11, pp. 1715-1720, November 1981
3. T. L. Carroll, "A Nonlinear Dynamics Method for Signal Identification," *An Interdisciplinary Journal of Nonlinear Science*, Vol. 17, pp. 023109, 2007
4. K. G. Gard, L. E. Larson, and M. B. Steer, "The Impact of RF Front-End Characteristics on the Spectral Regrowth of Communications Signals," *IEEE Transactions on Microwave Theory and Techniques*, Vol. 53, No. 6, pp. 2179-2186, Jun. 2005
5. G. Huang, Y. Yuan, X. Wang, and Z. Huang, "Specific Emitter Identification based on Nonlinear Dynamical Characteristics," *Canadian Journal of Electrical & Computer Engineering*, Vol. 39, No. 1, pp. 34-41, 2016
6. S. D'agostino, "Specific Emitter Identification based on Amplitude Features," in *Proceedings of IEEE International Conference on Signal and Image Processing Applications* (*ICSIPA*), pp. 350-354, October 2015
7. H. H. Ye, Z. Liu, and W. L. Jiang, "Comparison of Unintentional Frequency and Phase Modulation Features for Specific Emitter Identification," *Electronics Letters*, Vol. 48, No. 14, pp. 875-876, 2012
8. X. H. Ru, Z. Liu, W. L. Jiang, et al., "Recognition Performance Analysis of Instantaneous Phase and its Transformed Features for Radar Emitter Identification," *IET Radar Sonar and Navigation*, Vol. 10, No. 5, pp. 945-952, 2016
9. J. Dudczyk and A. Kawalec, "Fractal Features of Specific Emitter Identification," *Acta Physica Polonica A*, Vol. 124, No. 3, pp. 406-409, 2013
10. Y. Shi and H. B. Ji, "Kernel Canonical Correlation Analysis for Specific Radar Emitter Identification," *Electronics Letters*, Vol. 50, No. 18, pp. 1318-1320, 2014
11. J. Zhang, F. Wang, O. A. Dobre, et al., "Specific Emitter Identification via Hilbert–Huang Transform in Single-Hop and Relaying Scenarios," *IEEE Transactions on Information Forensics and Security*, Vol. 11, No. 6, pp. 1192-1205, 2016
12. N. Huang, and Z. Wu, "A Review on Hilbert‐Huang Transform: Method and its Applications to Geophysical Studies," *Reviews of Geophysics*, Vol. 46, No. 2, 2008
13. A. P. Pentland, "Fractal based Description of Natural Scenes," *IEEE Transactions on Pattern Analysis and Machine Intelligence*, Vol. 6, pp. 661-674, 1984
14. R. Li and Y. F. Hu, "Based on the Density of kNN Text Classifier Training Sample Cutting Method," *Computer Research and Development*, Vol. 41, No. 4, pp. 539-545, 2004